THE JOURNAL OF PHYSICAL CHEMISTRY B

Article

pubs.acs.org/JPCB

Full Color Modulation of Firefly Luciferase through Engineering with Unified Stark Effect

Duanjun Cai,*[,†,‡] Miguel A. L. Marques,[‡,§] and Fernando Nogueira[‡]

[†]Fujian Key Laboratory of Semiconductor Materials and Applications, Department of Physics, Xiamen University, Xiamen 361005, China

[‡]CFC, Departamento de Física, Universidade de Coimbra, 3004-516 Coimbra, Portugal

[§]Université de Lyon, F-69000 Lyon, France and LPMCN, CNRS, UMR 5586, Université Lyon 1, F-69622 Villeurbanne, France

Supporting Information

ABSTRACT: The firefly luciferase has been a unique marking tool used in various bioimaging techniques. Extensive color modulation is strongly required to meet special marking demands; however, intentional and accurate wavelength tuning has yet to be achieved. Here, we demonstrate that the color shift of the firefly chromophore (OxyLH$_2$-1) by internal and external fields can be described as a unified Stark shift. Electrostatic microenvironmental effects on fluorescent spectroscopy are modeled in vacuo through effective electric fields by using time-dependent density functional theory. A complete visible fluorescence spectrum of firefly chromophore is depicted, which enables one to control the emission in a specific color. As an application, the widely observed pH-correlated color shift is proved to be associated with the local Stark field generated by the trace water−ions (vicinal hydronium and hydroxide ions) at active sites close to the OxyLH$_2$-1.

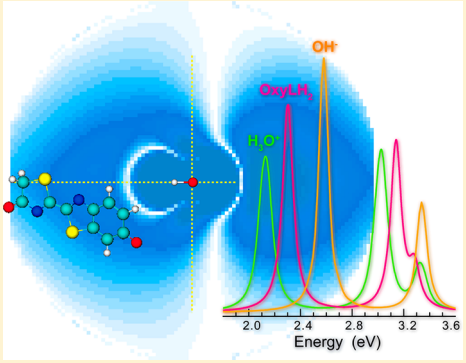

The firefly luciferin/luciferase system, a famous example of bioluminescent proteins, has been successfully used in various bioimaging techniques,[1] as a reporter for ATP generation[2] and gene expression,[3] and as a biosensor for environmental pollutants.[4] In all these diverse applications, some special marking demands require an extensive color modulation of the fluorescent properties of the protein. For this purpose, mechanisms resulting in or leading to color shift, color tuning, and brightness enhancement have been actively studied.[5,6] The spectral shifts of the protein fluorescence are thought to arise mainly from changes in local electrostatic interactions between the chromophore and the protein environment.[7,8]This can be understood as an "internal" Stark effect,[9] where the protein cavity field that is closely associated with the charged/polar amino termini plays the key role in shifting the emitting color. The external fields such as an applied electric field or the electrostatic field from polar solvent molecules introduce an "external" Stark effect. In the presence of an internal electric field $\vec{e}_C$ the spectral shift of chromophore fluorescence is given by:

$$E_A = E_{A0} - \Delta\vec{\mu} \times \vec{e}_C \quad (1)$$

where E_{A0} is the peak energy in the absence of electric field, and $\Delta\vec{\mu}$ represents the change of dipole moment between the ground and excited state. Additionally, $\Delta\vec{\mu}$ can be further split in two parts:[10] the intrinsic difference of the permanent dipole moments in the excited and the ground states, $\Delta\vec{\mu}_0 = \mu_x - \mu_g$, and the change induced by the electric field, $\Delta\vec{\mu}_e = \frac{1}{2}\Delta\vec{\alpha} \times \vec{e}_C$. Here, $\vec{\alpha}$ is the polarizability tensor of the chromophore molecule. Inserting $\Delta\vec{\mu}$ into eq 1, one obtains the second-order internal Stark shift

$$E_A = E_{A0} - \Delta\vec{\mu}_0 \times \vec{e}_C - \frac{1}{2}\vec{e}_C \times \Delta\vec{\alpha} \times \vec{e}_C \quad (2)$$

Usually, the second-order Stark shift only gives a significant contribution for a very large electric field and is usually neglected. Recently, experimental measurements of the dipole moment[11] and also some theoretical calculations[12] revealed the existence of a quadratic Stark shift in fluorescent proteins due to the internal electrostatic interaction. These studies seem to indicate that the magnitude of the electric field generated by the protein is of the order of tens of MV/cm,[13] similar to the external fields that can be applied experimentally. Clearly, a unification of the internal and external Stark effects can then be made, with a corresponding simplification of its use in mutagenesis techniques for the color tuning of luciferase and fluorescent proteins.

In long-term color tuning studies, one of the most frequently used chemical factors, namely pH, was found to have a distinct influence on the color shift. It has been widely reported that a red shift of luminescence occurs with a lower pH, whereas a blue shift comes up at higher pH.[14] In particular, when

Received: June 8, 2013
Revised: September 27, 2013
Published: October 2, 2013

quantitatively re-examining the quantum yield of firefly bioluminescence, Ando and his coauthors observed that the spectral line shape at about 2.2 eV is extremely pH-sensitive and proposed that this simple intensity variation could be the real reason for the color change.[15] However, due to the difficulties in determining the configuration of the hydrogen atoms and the complexity of solvent effects, the mechanism responsible for these interesting phenomena remains ambiguous, and explanations are elusive. Since the electrostatic interaction has the leading role in color shift and water ions are charged molecules, it is believed that the pH-related spectral shift and deformation may also be expressed in the language of a unified Stark effect.

In this work, the color shift of the firefly chromophore by internal and external fields is described as a unified Stark shift. Electrostatic microenvironmental effects on fluorescent spectroscopy were modeled through effective electric fields by using time-dependent density functional theory (TDDFT). The parameters for the first- and second-order Stark effects are determined, and a complete visible fluorescence spectrum of firefly chromophore is depicted, which enables one to intentionally and accurately tune it in order to emit in a specific color. As an application, the widely observed pH-correlated color shift was investigated by considering the Stark field generated by trace water−ions enclosed in the protein. We found that the distinct Stark effect on the chromophore with the vicinal water−ions, hydronium, and hydroxide at active sites is the main reason leading to the spectral shift and deformation at different pH.

The chromophore of the firefly luciferase, oxyluciferin ($OxyLH_2$), is located in the central part of a protein pocket and is surrounded by several side chains and solvent molecules,[16,17] as shown in Figure 1a. Detailed studies of the firefly chromophores in both bioluminescence and chemiluminescence suggested that the keto-form $OxyLH_2$ is one of the most important light emitters responsible for the fluorescence.[18,19] Therefore, the $OxyLH_2$ in its deprotonated keto(-1) form [$OxyLH_2$-1] was considered in this work, based on the X-ray structure of the Japanese firefly luciferase (*Luciola cruciata*, PDB database code: 2d1r). The background of the chromophore is a vacuum, and the solvent effect by using the dielectric constant was not involved. TDDFT calculations were carried out using the octopus code.[20,21] Exchange-correlation effects were treated, adiabatically, within the local-density approximation.[22,23] A uniform grid spacing of 0.20 Å, a sphere radius of 5.0 Å, and a time step of 0.001 fs were used to ensure the stability of the time-dependent propagation and leading to spectra with a resolution better than 0.1 eV. The total charges of the model are defined by using the parameter of excess charges in our calculations. Although absorption is different from light emission, the absorption spectrum could basically represent the main properties of the optical process. The emission spectrum has been calculated with the optimized geometry at the first excited state and compared with the absorption spectrum (see Supporting Information). A distinguishable systematic red shift appears in the two main emission peaks with respect to the absorption ones, and meanwhile, the emission peak has a lower intensity (oscillator strength), which is due to the nonradiative decay rate (~23%).

As mentioned previously, eq 2 only describes the internal Stark shift induced by the protein cavity field. If we take into account this cavity field together with any existing external fields (such as the electrostatic field from polar solvent molecules), the entire environmental electrostatic interactions can then be regarded as an effective external electric field imposed on the chromophore, as represented in Figure 1b. This electric field $f\vec{e}$ is a superposition of the internal $\vec{e}_C$ and the effective external $f\vec{e}_S$ fields,

$$f\vec{e} = \vec{e}_C + f\vec{e}_S \tag{3}$$

Here, f stands for an effective field factor which takes into account the modification of the external field at the site of the chromophore, through the protein cavity. In the case of an internal field, $f = 1$. For convenience, we define an orthogonal coordinate system with respect to the chromophore molecule configuration with three perpendicular directions (Figure 1b): x along the long molecular axis, y along the short axis, and z normal to the molecular plane. Thus, any type of environmental electric fields can be decomposed into components projected on these three coordinate directions. Hence, a universal expression of the Stark effect is obtained by replacing $\vec{e}_C$ in eq 2 with $f\vec{e}$:

$$E_A = E_{A0} - \sum_{i,j=1}^{3} \left(f\Delta\mu_{0,i} \times e_i - \frac{1}{2} f^2 e_i \cdot \Delta\alpha_{ij} \times e_j \right) \tag{4}$$

where i and j represent the projected field on x, y, or z direction. The parameters in eq 4 can be calculated by imposing electrostatic fields e_i onto $OxyLH_2$-1 in each of the perpendicular directions, and a complete color shift map can be obtained. Uniform fields were used, and the magnitude of these fields was considered to be close to the environmental electric field around $OxyLH_2$-1 in the protein cavity (i.e., ~150 mV/Å, see Supporting Information). We found that the Stark shift under e_z (out of the molecule plane) is negligibly small. This is because the polarizability and dipole moments associated with the excitations are mainly oriented within the

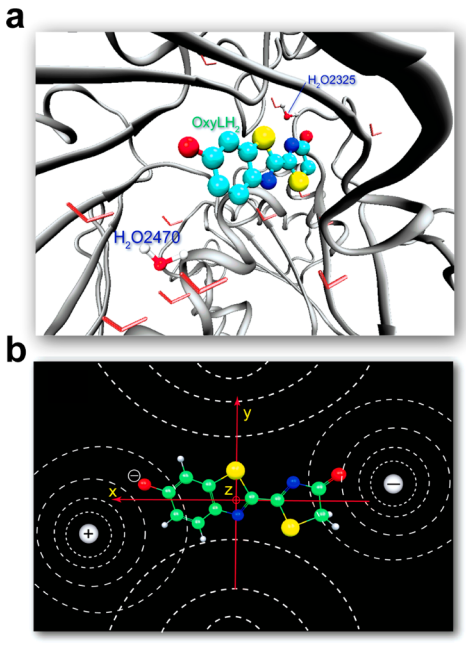

Figure 1. (a) Firefly protein structure with chromophore $OxyLH_2$-1 and water molecules in the pocket. (b) Schematic of the coulomb interaction, which can be represented by the effective electrostatic fields. Three perpendicular axes x, y, and z are defined.

dx.doi.org/10.1021/jp405665v | J. Phys. Chem. B 2013, 117, 13725−13730

$OxyLH_2$-1 plane.[13] Thus, we only need to focus on the change introduced by e_x and e_y, as shown in Figure 1b.

In the absorption spectra, two main peaks A1 and A2 can be identified, and the A2 peak comprises two subpeaks, A2-1 and A2-1. The A1 peak is assigned dominantly to the HOMO→LUMO transition, whereas the A2 peak is due essentially to the HOMO-2→LUMO transition.[24] When an electric field is applied, the Stark effect leads to a wavelength shift as well as a line shape deformation of the spectra. Negative values of e_x or e_y give rise to a blue shift of A1, whereas positive values lead to a red shift. Detailed examination shows that the energetic shift is mainly attributed to the shift of the HOMO under electric fields. For the A2 peaks, this shift is clearly quadratic in the applied field, reflecting the effect of the second-order Stark shift. By fitting with eq 4, coefficients were determined and summarized in Table 1 for different absorption peaks. The

Table 1. Coefficients for the Unified Stark Shift in Eq 4 by Fitting with the Spectral Shift in the Presence of Applied Equivalent Electric Fields[a]

coefficient	E_{A1} (e_x)	E_{A1} (e_y)	$E_{A2\text{-}1}$ (e_x)	$E_{A2\text{-}1}$ (e_y)	$E_{A2\text{-}2}$ (e_y)
E_{A0} (eV)	2.34	2.34	3.21	3.18	3.34
$f\Delta\mu_0$ (eÅ)	0.364	0.30	0.55	−0.145	−0.185
$f^2\Delta\alpha$ (eÅ²/V)	0.022	0.19	−0.13	0.08	0.056
$\mu_x - \mu_g$ (eÅ)	0.335	0.294	0.824	−0.158	−0.217

[a]The dipole moment difference, $\mu_x - \mu_g$, in the absence of electric fields is obtained by direct calculation, showing good consistency with the fitting value $\Delta\mu_0$.

calculated $\mu_x - \mu_g$ in the absence of applied fields is consistent with the fitting value $\Delta\vec{\mu}_0$ ($f = 1$). The second-order (quadratic) coefficients $f^2\Delta\alpha$ show a more significant influence on the E_{A1} peak under e_y field and the E_{A2} peak under e_x field, indicating the sensitivity of these two optical excitations. Of course, the quadratic effect becomes considerable only under strong Stark field while the linear shift dominants under normal fields (with magnitude smaller than 40 mV/Å).

As the first absorption A1 peak represents the main firefly light emission, we computed the 2D color map of the wavelength shift of A1 as a function of Stark fields e_x and e_y (Figure 2). Colors in the full visible band are covered in the map, and the light outside this range could also be obtained simply by outward extension. According to this map, a full color tuning of firefly chromophore emission can be intentionally operated by: (1) choosing the desired color (wavelength) and finding its position in this map; (2) reading the corresponding Stark field e_x and e_y, for which one may have several choices because the color in a certain wavelength appears as an oblique stripe; (3) searching for the suitable type of amino acid (charged or polarized) and the point of insertion in the protein chain, which ultimately could generate these e_x and e_y fields on the $OxyLH_2$-1, as predicted in step (2). By these means, accurate color tuning of the firefly chromophore could be achieved practically through mutagenesis. To examine the accuracy of this method, we selected important charged residues in the nearest shell of $OxyLH_2$-1, such as Lys531, Arg339, His247, among others, and calculated the induced spectral shifts due to their Stark fields on the $OxyLH_2$-1 site (detailed in Supporting Information). Here we used the neutral keto(0) form $OxyLH_2$-1, the E_{A1} of which is about 2.95 eV, to determine the accuracy of the estimation by Stark shift. From Table 2, one can see that the comparison with the estimated

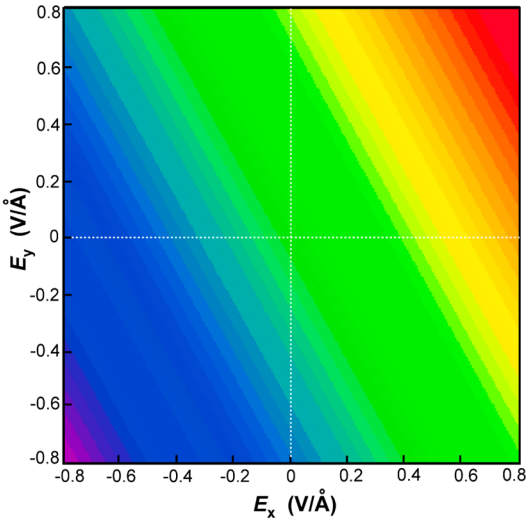

Figure 2. Color map as a function of electrostatic fields e_x and e_y. Intentional color tuning can be achieved by locating desired emitted wavelength in this map.

value shows a good consistency, suggesting the usability of the color tuning method. It is further confirmed that the equation of the unified Stark shift can correctly estimate the shift of wavelength with a given electric field stemmed from the side groups or external fields. One can see that the estimated value of Stark shift E is accurately consistent (~0.01 eV) with the spectral energy. We would like to emphasize here that parameters such as charge sign, amount, distance, and angle of charged residues are of importance in determining the light wavelength. These data are crucial and useful for future structural design of the fluorescence of the firefly chromophore, and this table will be extended in the future by completing the missing data for other residues and molecules.

The aforementioned results clearly demonstrate that the charged ions or molecules are the most active factors influencing the luminescence color. Besides the color shift, the peak intensity variation and line shape deformation in Figure 3 cannot be ignored as well, which is especially significant for the A2 doublet peaks. The A2-1 peak intensity is largely suppressed with negative e while the oscillation strength of A2-2 is enhanced. This variation results in a behavior of the doublet split and main wavelength swapping. This phenomenon appears very similar to the assumption by Ando and coworkers that the pH-dependent color shift may be due to spectral variation controlled by other factors other than the molecular form switching between keto and enol states.[15] In this regard, the dominant factor apparently points to the Stark field, while the critical problem here is how to build the link to the conventional pH value.

In general, the pH value measures the macroscopic activity (concentration) of water ions (i.e., hydrogen ions and hydroxide ions). The pH arises due to the relatively local interaction between these active ions and the host molecule in the solvent. As discussed previously, the charged residues as well as buried water ions will largely contribute to the Stark field at the $OxyLH_2$-1 site. This suggests that, as shown in Figure 1a, the location and electrostatic field of hydronium ion H^+ and/or hydroxide ion OH− is tightly associated with the color shift at different pH. According to the "Zundel" or "Eigen" model,[25,26] the $H_5O_2^+$ or $H_9O_4^+$ complexes are the relevant forms of hydronium ion in liquid water, while in trace

dx.doi.org/10.1021/jp405665v | J. Phys. Chem. B 2013, 117, 13725−13730

Table 2. Stark Shifts of Selected Important Residues in the First Shell around the Chromophore $OxyLH_2$ [Keto(0) Form] in the Firefly Protein Side Chain[a]

residue	charge	group	d (Å)	(x, y) (Å)	(e_x, e_y) (mV/Å)	E_{A1} (eV)	Γ_{A1} (eV)	E_{A2} (eV)	Γ_{A2} (eV)
Lys531	+1	ε -amino	5.15	(−8.2, 5.1)	(59.1, −1.8)	2.78	2.77	3.13	3.13
Lys531-0	0	ε -amino	5.15	(−8.2, 5.1)	(−0.45, −2.0)	2.95	2.96	3.32	3.33
Arg339	+1	guanidinium	6.17	(10.5, −0.34)	(−52.9, −14.2)	2.98	3.08	3.50	3.50
Arg220	+1	guanidinium	4.69	(4.01, −5.74)	(−56.9, 17.6)	2.96	3.05	3.52	3.50
His247	+1	imidazole ring	4.54	(−5.9, 0.32)	(103, 19.3)	2.57	2.57	3.01	3.01
His247-0	0	imidazole ring	4.54	(−5.9, 0.32)	(8.5, 0.97)	2.93	2.92	3.29	3.30
Glu346	−1	carboxylate anion	8.07	(−11.9, −1.52)	(−79.6, −44)	2.96		3.59	
His223	+1	imidazole ring	9.62	(2.59, −6.97)	(−19, 7.8)	2.97	2.98	3.39	3.42
AMP	−2	phosphate anion	3.27	(−8.57, 1.94)	(−195, −85.8)	2.52		4.07	
H_2O no. 2470	0	water molecule	4.42	(7.12, −3.63)	(−8.9, −1.3)	2.96	2.97	3.35	3.35
H_2O no. 2325	0	water molecule	3.33	(−5.66, 4.1)	(−6.7, −2.7)	2.96	2.97	3.34	3.34

[a]The charge, group type, distance d between the each residue and $OxyLH_2$, position (x, y), induced Stark field on the $OxyLH_2$ site, predicted peak energy E with Stark shift by eq 4, and the calculated spectral energy Γ of $OxyLH_2$ with interaction with each residue are listed. By comparing the values of E and Γ, the accuracy of Stark shift obtained with eq 4 is confirmed.

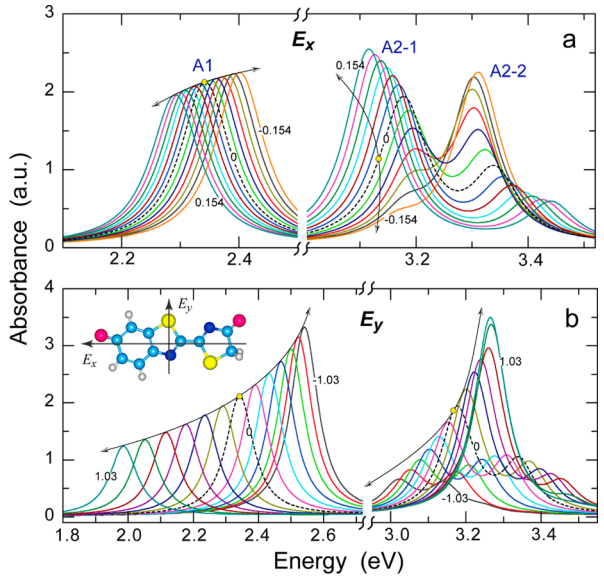

Figure 3. Absorption spectra of $OxyLH_2$-1 as a function of the local electrostatic fields along e_x (a) and e_y (b), respectively, in units of V/Å. The inset shows the definition of two perpendicular directions in the molecular plane.

water environment, the preferable hydronium ion structure should still be H_3O^+ (see Supporting Information). The electrostatic fields generated by the neutral water molecule and its cation/anion were calculated and displayed in Figure 4. Due to the polarized orientation and hydrogen-bond coordination, the surrounding electric fields of water, H_3O^+, and OH− appear in different shapes: butterfly like, dumbbell-like, and dual-peach-like, respectively. As shown in Figure 4a, the negative electric field from H_2O merely exists within a radius of a few Angströms and then drops rapidly, indicating a short-range electrostatic interaction. On the side where the two hydrogen legs lay, there is a 30° sector where the electric field becomes very weak, which can be attributed to the dipole cancellation effect in this polar molecule. Thus, the electrostatic interaction between water and nearby molecules becomes strongly orientation-dependent. In contrast, the H_3O^+ ion generates a long-range positive field along x and y (Figure 4c), extending much further than that of neutral H_2O. The similar sector of weak-field area again appears while it opens up an angle of only 21.6° on both sides between the two dumbbells. As a comparison, the electric field from the $H_5O_2^+$ ion (Figure 4d) shows the similarity of the magnitude and shape to that from H_3O^+. This explains that in the trace water case, the complex of hydronium ion does not change appreciably the type and distribution of the electrostatic field. The most complicated field distribution appears in a dual-peach shape for the OH^- anion (Figure 4b), which illustrates the strong inequivalence along two axes; although the effective range in $\pm x$ reaches 9 Å, the e_y extends only less than half that far. A 99.1° active sector can be defined for the right "peach", and the weak-field area covers widely (white and light blue area) in the upper and lower space. In particular, the dipole cancellation effect results in a special pair of "C" and reflected "C" shaped zero-field arcs encircling the OH^- molecule.

To confirm the hypothesis of the Stark shift by active water ions, the water molecule, hydronium, and hydroxyl ions were introduced onto the preferable active sites close to the $OxyLH_2$-1 inside the protein cavity, as shown in Figure 1a. The most important sites were found to be no. 2325 and no. 2470, which lie at the two ends of $OxyLH_2$-1 along the polarization orientation (x-axis). The geometries (including hydrogens) of H_2O, H_3O^+, OH^-, and $OxyLH_2$-1 were optimized, and the final absorption spectra of $OxyLH_2$-1 were plotted in Figure 5. The influence on the color or spectral shape by the neutral water molecules is negligibly small (slight blue shift, < 0.05 eV), due to their weak electric field (Figure 4a). This means that the argument put forth before[6] about the major role played by the H-bond network of waters in the cavity on the color shift does not seem to hold. Instead, the Stark field generated by the water−ions associated with the pH states may take over this role.

The H_3O^+ ion formed in a low pH environment prefers to reside at site no. 2325 (see Supporting Information), which is at a distance of 7.9 Å from $OxyLH_2$-1 and at 12° outside the forbidden sector (Figure 4c). Thus, the positive electrostatic interaction leads to a red shift of about 0.2 eV for the $OxyLH_2$-1 A1 peak and about 0.1 eV for the A2 main peak, as shown in Figure 5. In addition, a split of the A2 doublet peaks appears, and the energetic separation between the two subpeaks increases up to ~0.3 eV. This demonstrates the clear origin of the low pH red shift and line shape variation. On the contrary, the no. 2470 OH^- ion at higher pH locates at the site close to the deprotonated O in the benzothiazole ring (Figure

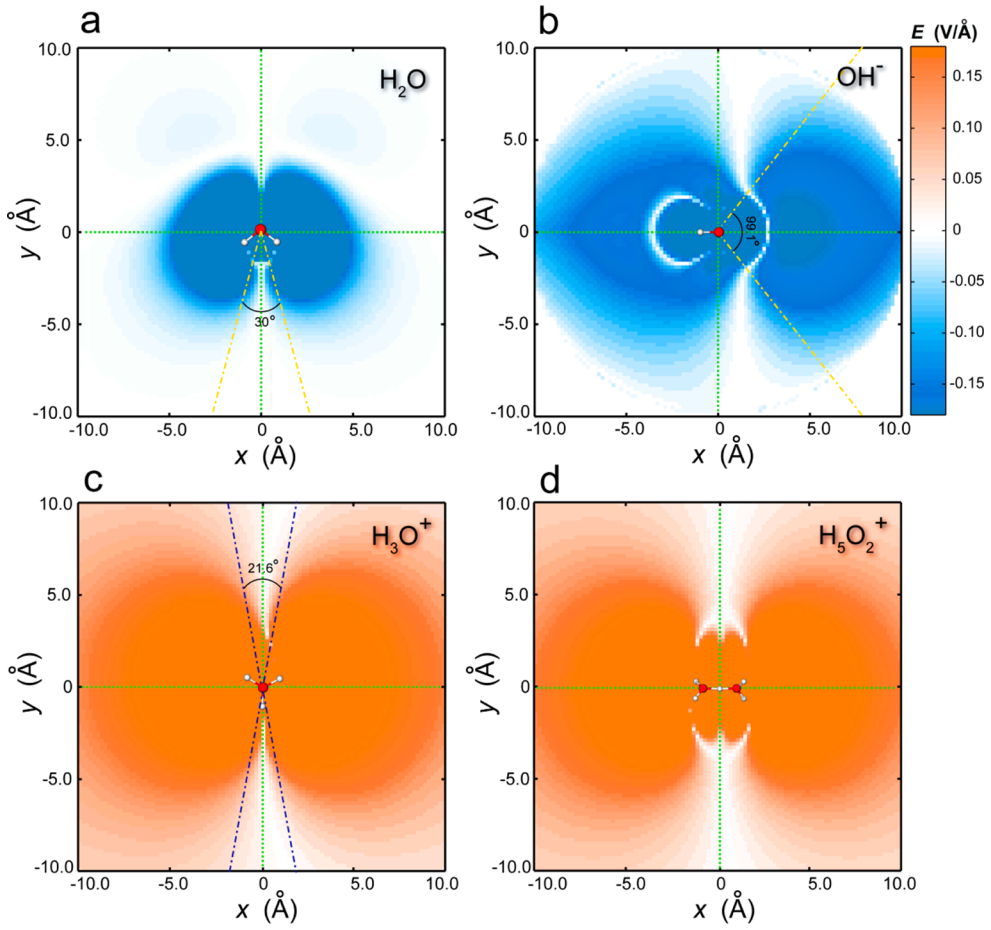

Figure 4. Distribution of electrostatic fields around water ions. That for the H_2O (a), OH^- (b), H_3O^+ (c), and $H_5O_2^+$ (d) shows a shape of butterfly like, dumbbell-like, and dual-peach-like, respectively. The sector angles indicating the area of field absence and the interaction region are marked.

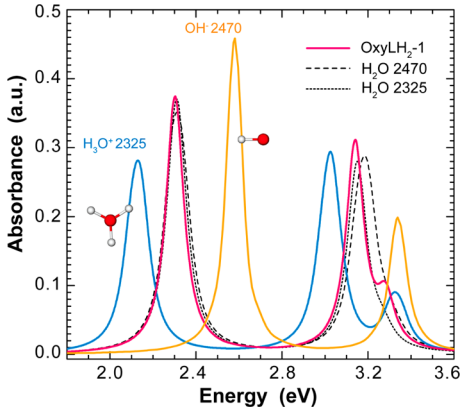

Figure 5. Stark shift of the emitting spectrum of OxyLH$_2$-1 in the protein pocket containing active water molecules at special sites (no. 2325 and 2470) and/or their ions.

1a), which results in a significant blue shift of A1 by 0.27 eV with respect to the emission in neutral solvent, accompanied by a strong enhancement of the emission intensity by 24%. As reported by Wang and their co-workers, the spectra of the WT Lcr and Y257F mutant will undergo a red shift, and the peak intensity decreases as the pH value decreases,[27] which is consistent with our results. The strong pH sensitivity of the color shift and the subpeak intensity below pH 8.0[15] can be well-explained. The blue shift with increasing pH actually stems from the Stark shift as well as the increase of peak intensity, rather than from a simple intensity variation. Now we know that what the pH value indicates is a solvent environment with different water−ion concentrations, under which a trace of water−ions will enter the protein cavity and settle at favorable sites. The distance and orientation angle of the water−ions with respect to OxyLH$_2$-1 determines the quantitative strength of electrostatic field action on the color shift and spectral deformation. An accurate determination of the structure and distribution of pocketed water−ions in fluorescent luciferase as a function of pH is therefore needed to fully understand the effect of pH on firefly luminescence. We note that there also exists another case such as those pH-insensitive luciferases or mutants,[27] in which the water ions have much lower probability to access the protein cavity or to arrive at those crucial active sites. That is why the luminescent spectrum could be insensitive to the pH change.

In conclusion, the Stark shift unifies the color shift of the fluorescent chromophore by internal and external fields, which allows the complete scan of the absorption and emission as a function of the electrostatic field using TDDFT. For the firefly luciferase, the determination of the first- and second-order coefficients in the Stark equation suggests that intentional color tuning over the complete visible range could be accurately achieved. Furthermore, the widely observed pH-correlated color shift was proven to be associated with the local Stark field generated by the trace water−ions close to the OxyLH$_2$-1. The distinct Stark effect on the chromophore, with the vicinal

dx.doi.org/10.1021/jp405665v | J. Phys. Chem. B 2013, 117, 13725−13730

hydronium and hydroxide ions at active sites, was found to be the main reason resulting in the spectral shift and deformation at different pH states. This approach can be applied to various luciferases and fluorescent proteins and to guide the functionalization of organic optoelectronic devices.

■ ASSOCIATED CONTENT

Supporting Information

Geometry information, evaluation of electrostatic fields around the chromophore molecule, determination of the Stark shifts by neighboring residues in a complete table, and detailed description of critical water−ions. This material is available free of charge via the Internet at http://pubs.acs.org.

■ AUTHOR INFORMATION

Corresponding Author

*E-mail: dcai@teor.fis.uc.pt.

Notes

The authors declare no competing financial interest.

■ ACKNOWLEDGMENTS

The authors thank the CFC of the University of Coimbra and the Milipeia supercomputer system for providing CPU time. This work was partly supported by the "973" programs (2012CB619301 and 2011CB925600) and "863" (2011AA03A111), the FRFCU (2012121011 and 2011121042), and the NNSF (61204101) of China.

■ REFERENCES

(1) Viviani, V. R. The origin, diversity, and structure function relationships of insect luciferases. *Cell. Mol. Life Sci.* **2002**, *59*, 1833−1850.

(2) Chalfie, M.; Tu, Y.; Euskirchen, G.; Ward, W. W.; Prasher, D. C. Green fluorescent protein as a marker for gene expression. *Science* **1994**, *263*, 802−805.

(3) Pierce, D. W.; Hom-Booher, N.; Vale, R. D. Imaging individual green fluorescent proteins. *Nature* **1997**, *388*, 338.

(4) Nakatsu, T.; Ichiyama, S.; Hiratake, J.; Saldanha, A.; Kobashi, N.; Sakata, K.; Kato, H. Structural basis for the spectral difference in luciferase bioluminescence. *Nature* **2006**, *440*, 372−376.

(5) Branchini, B. R.; Southworth, T. L.; Murtiashaw, M. H.; Magyar, R. A.; Gonzalez, S. A.; Ruggiero, M. C.; Stroh, J. G. An alternative mechanism of bioluminescence color determination in firefly luciferase. *Biochemistry* **2004**, *43*, 7255−7262.

(6) Navizet, I.; Liu, Y. J.; Ferre, N.; Xiao, H. Y.; Fang, W. H.; Lindh, R. Color-tuning mechanism of firefly investigated by multi-configurational perturbation method. *J. Am. Chem. Soc.* **2009**, *132*, 706−712.

(7) Henderson, J. N.; Remington, S. J. Crystal structures and mutational analysis of amFP486, a cyan fluorescent protein from Anemonia majano. *Proc. Natl. Acad. Sci. U.S.A.* **2005**, *102*, 12712−12717.

(8) Ai, H. W.; Olenych, S. G.; Wong, P.; Davidson, M. W.; Campbell, R. E. Hue-shifted monomeric variants of Clavularia cyan fluorescent protein: Identification of the molecular determinants of color and applications in fluorescence imaging. *BMC Biol.* **2008**, *6*, 13.

(9) Lockhart, D. J.; Kim, P. S. Internal stark effect measurement of the electric field at the amino terminus of an alpha helix. *Science* **1992**, *257*, 947−951.

(10) Berlin, Y.; Burin, A.; Friedrich, J.; Kohler, J. Spectroscopy of proteins at low temperature. Part I: Experiments with molecular ensembles. *Phys. Life Rev.* **2006**, *3*, 262−292.

(11) Drobizhev, M.; Tillo, S.; Makarov, N. S.; Hughes, T. E.; Rebane, A. Color hues in red fluorescent proteins are due to internal quadratic Stark effect. *J. Phys. Chem. B* **2009**, *113*, 12860−12864.

(12) Cai, D.; Marques, M. A.; Nogueira, F. Accurate color tuning of firefly chromophore by modulation of local polarization electrostatic fields. *J. Phys. Chem. B* **2011**, *115*, 329−332.

(13) Manas, E. S.; Wright, W. W.; Sharp, K. A.; Friedrich, J.; Vanderkooi, J. M. The influence of protein environment on the low temperature electronic spectroscopy of Zn-substituted cytochrome c. *J. Phys. Chem. B* **2000**, *104*, 6932−6941.

(14) Branchini, B. R.; Ablamsky, D. M.; Rosenman, J. M.; Uzasci, L.; Southworth, T. L.; Zimmer, M. Synergistic mutations produce blue-shifted bioluminescence in firefly luciferase. *Biochemistry* **2007**, *46*, 13847−13855.

(15) Ando, Y.; Niwa, K.; Yamada, N.; Enomot, T.; Irie, T.; Kubota, H.; Ohmiya, Y.; Akiyama, H. Firefly bioluminescence quantum yield and colour change by pH-sensitive green emission. *Nat. Photonics* **2008**, *2*, 44−47.

(16) Nakatsu, T.; Ichiyama, S.; Hiratake, J.; Saldanha, A.; Kobashi, N.; Sakata, K.; Kato, H. Structural basis for the spectral difference in luciferase bioluminescence. *Nature* **2006**, *440*, 372−376.

(17) Finkelstein, J. Chemical biology: A pocketful of colour. *Nature* **2006**, *440*, 285.

(18) Li, Z. W.; Ren, A. M.; Guo, J. F.; Yang, T.; Goddard, J. D.; Feng, J. K. Color-tuning mechanism in firefly luminescence: Theoretical studies on fluorescence of oxyluciferin in aqueous solution using time dependent density functional theory. *J. Phys. Chem. A* **2008**, *112*, 9796−9800.

(19) Nakatani, N.; Hasegawa, J. Y.; Nakatsuji, H. Red light in chemiluminescence and yellow-green light in bioluminescence: Color-tuning mechanism of firefly, *Photinus pyralis*, studied by the symmetry-adapted cluster-configuration interaction method. *J. Am. Chem. Soc.* **2007**, *129*, 8756−8765.

(20) Lopez, X.; Marques, M. A.; Castro, A.; Rubio, A. Optical absorption of the blue fluorescent protein: A first-principles study. *J. Am. Chem. Soc.* **2005**, *127*, 12329−12337.

(21) Marques, M. A. L.; Castro, A.; Bertsch, G. F.; Rubio, A. Octopus: A first-principles tool for excited electron-ion dynamics. *Comput. Phys. Commun.* **2003**, *151*, 60−78.

(22) Hohenberg, P.; Kohn, W. Inhomogeneous electron gas. *Phys. Rev.* **1964**, *136*, B864−B871.

(23) Perdew, J. P.; Zunger, A. Self-interaction correction to density-functional approximations for many-electron systems. *Phys. Rev. B* **1981**, *23*, 5048−5079.

(24) Cai, D. J.; Marques, M. A. L.; Milne, B. F.; Nogueira, F. Bioheterojunction effect on fluorescence origin and efficiency improvement of firefly chromophores. *J. Phys. Chem. Lett.* **2010**, *1*, 2781−2787.

(25) Zundel, G.; Metzger, H. Z. *Physik. Chem. (N.F.)* **1968**, *58*, 225−245.

(26) Eigen, M. *Angew. Chem., Int. Ed. Engl.* **1964**, *3*, 1−19.

(27) Wang, Y.; Akiyama, H.; Terakado, K.; Nakatsu, T. Impact of site-directed mutant luciferase on quantitative green and orange/red emission intensities in firefly bioluminescence. *Sci. Rep.* **2013**, *3*, 2490−2495.